Droplet size and morphology characterization for diesel sprays under atmospheric operating conditions

V.Stetsyuk[1,*], J. E. Turner[1], C. Crua[1], R. Pearson[2], M. Gold[2]
[1] Centre for Automotive engineering, University of Brighton, UK
[2] BP Formulated Products Technology, Pangbourne, UK

Abstract

The shape of microscopic fuel droplets may differ from the perfect sphere, affecting their external surface area and thus the heat transfer with the surrounding gas. Hence there is a need for the characterization of droplet shapes, and the estimation of external surface area, in order to enable the development of physically accurate mathematical models for the heating and evaporation of diesel fuel sprays. We present ongoing work to automatically identify and reconstruct the morphology of fuel droplets, primarily focusing in this study on irregularly-shaped, partially-deformed and oscillating droplets under atmospheric conditions. We used direct imaging techniques based on long-working distance microscopy and ultra-high-speed video to conduct a detailed temporal investigation of droplet morphology. We applied purpose-built algorithms to extract droplet size, velocity, volume and external surface area from the microscopic ultra-high-speed video frames. High resolution images of oscillating droplets and a formation of a droplet form ligament, sphericity factors, volume as well as external surface area are presented for 500 bar injection pressure in the near nozzle region (up to 0.7 mm from nozzle exit) under atmospheric conditions. We observed a range of different liquid structures, including perfectly spherical, non-spherical droplets and stretched ligaments. We found that large droplets and ligaments exceeding the size of the nozzle hole could be found at the end of injection. In order to estimate droplet volume and external surface area from two-dimensional droplet information, a discrete revolution of the droplet silhouette about its major centroidal axis was used. Special attention was paid to the estimation of actual errors in the prediction of volume and surface characteristics from a droplet silhouette. In addition to the estimation of droplet volume and external surface area, the actual shape reconstruction in 3D coordinates from a droplet silhouette was performed in order to enable future numerical modelling studies of real droplets.

Keywords: Spray, atomization, droplets, morphology, imaging diagnostics

Introduction

It is typically considered that a primary anthropogenic source of important pollutants is the combustion of fossil fuel in different combustion devices. Main pollutants emitted from virtually all types of transportation and electric power generation stations are nitrogen oxides, carbon monoxide, unburned hydrocarbons and soot. Injection system employed in internal combustion engines is a key element in design of current and future diesel engines due to a number of reasons. The introduction of the liquid fuels inside a combustion chamber in a diesel engine is performed separately from the supply of air, which is already present in a cylinder. A typical diffusion flame is formed and the combustion rate is governed by the mixing time, because the chemical reaction time is very short, of the order of 2-5 ms. Since, fuel is introduced in a liquid state, evaporation must take place before efficient mixing can occur. The fuel injection is a complex process and has been the subject of experimental and theoretical investigation. The relationship between the combustion process and the spray parameters has been investigated, e.g. by [1-6]. Experimental characterization, i.e. the distribution of droplets sizes, characterization of individual droplets at the spray periphery, entire spray statistics of diesel spray formation were studied, e.g. by a number of authors [7-11]. The most traditional approaches to measure droplet sizes in spray system were based on Phase Doppler Anemometry (PDA)/Phase Doppler Particle Analyzer (PDPA) [12] and diffraction-based granulometer [13]. An important drawback of these techniques is inability to measure non-spherical droplets and highly deformed liquid structures. As it has been demonstrated, highly deformed droplets and irregular liquid structures can be observed during injection processes [14, 15]. Direct imaging techniques are suitable tools that can be used to capture all liquid structures with adequate spatial resolution. High resolution long-working distance microscopic imaging, which belongs to direct imaging methods, has been proved to be a valuable tool in understanding of droplets formation and breakup processes.

A detailed characterization of droplet morphology is necessary in order to develop appropriate computational models. The modelling of droplet collision, evaporation and ligament evolution requires experimental data of sufficiently good quality. Two-dimensional images obtained by using high resolution microscopic imaging, in principle, can provide detailed information about a range of liquid structures. However, the 2D images are formed of individual projected areas of 3D shapes. The same projected area can represent different liquid structures in object plane.

Traditionally, particle shape analyses are performed based on the assumption that particles are spherical. A number of pixels representing a droplet shape can be determined and equivalent diameter is computed in a straightforward manner. External surface area and volume of individual droplets can then be computed analytically [16]. The assumption of sphericity may not be valid for all operating conditions and injection phases. During idle engine load, the injection pressure is low and high non-spherical droplets are expected to be found. In this work it is demonstrated that during droplet life time, the droplet morphology could be quite different due to external forces acting on the droplet. Distribution of drop sizes in high pressure fuel sprays is influenced by drag forces due to droplets high velocity. Drop distortion and oscillation result in dynamic change of drag coefficient, which should be taken into account by numerical models.

Liquid spray droplet morphology was investigated by, e.g. [17, 18] by using various criterions. Estimation of droplet volume from 2D imaging techniques was outlined, e.g. by [19]. An excellent overview of spray measurements technology is also given by [20]. At present, experimental data at engine conditions for oscillating droplet morphology and droplet formation from ligaments is particularly limited, which is crucial to estimating of droplet breakup mechanisms. Therefore, the main goal of the present work is to estimate morphology of oscillating droplets and ligaments during the end of injection by using discrete revolution method, which was suggested by [16]. This approach relies on a principle of discrete revolution about major centroidal axis of individual slices of a sliced object. In fact, discrete revolution method uses 2D images to create 3D representation of a two-dimensional object. The major centroidal axis is the axis, which passes through the centre of gravity of an object and about which moment inertia of the object is minimized. For a simple geometrical shape, such as a long cylinder, which is represented as a rectangle with long sides on 2D images, the major centroidal axis is along the longest side. The detailed description of this method can be found in [16].

The remaining paper is structured as follows: The next section outlines experimental setup, which was used to investigate droplet morphology under atmospheric operating conditions. Then, main findings are outlined. The paper ends with the summary of the main conclusions.

Experimental setup

The ultra-high-speed microscopy setup used by the authors at the University of Brighton is described in [21], hence only a brief description will be included here. The diesel liquid spray investigated under atmospheric conditions was produced by a conventional 7-hole diesel fuel injector DFI 1.5 with nominal nozzle diameter of 0.135 mm. The injector was mounted in an atmospheric chamber horizontally perpendicular to a light source and a high speed camera (Figure 1). The illumination of the sprays was achieved by a 500 joule xenon flashgun, which delivered a 2 ms light pulse synchronized with a CCD camera. Ultra-high speed intensified CCD camera SIM16 from Specialised Imaging Ltd. was used to capture 16 images at a rate of 200,000 frames per second. The camera exposure was set to 500 ns. All images were taken at 1.0 ms ASOI. The camera was equipped with a long-distance microscope with a nominal working distance of 95 mm and numerical aperture of 0.204. The camera was synchronized with an injection event via a programmable pulse generator. Injection pressure was 500 bar, which was representative of idle engine load. The injection duration was 500 μs. The fuel was ordinary diesel fuel with no bio content B0. A conventional common-rail injection system was employed with a number of classical components.

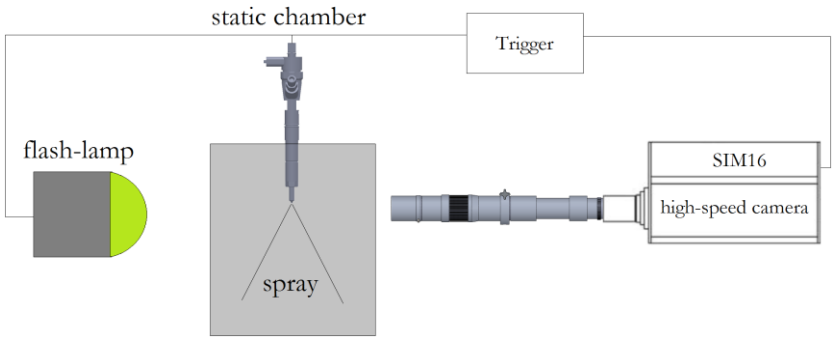

Figure 1: Experimental setup used to study droplet morphology under atmospheric conditions. SIM16 camera was equipped with a long-working distance microscope. The field of view for the microscope was within 0.5 mm from the injector nozzle.

Raw images were binarised by using a threshold method and projected area, sphericity parameter, estimated volume as well as estimated external surface area were computed. The sphericity parameter, which quantifies the likeness between the droplet shape and the spherical shape, was computed according to Blaisot [18] as follows:

$$S_p = \frac{area\left(S_I \cup S_C - S_I \cap S_C\right)}{area\left(S_I\right)}, 0 < S_p < 2 \quad (1)$$

where: S_p sphericity parameter ($S_p = 0$ for spherical droplet), S_I is area of the droplet image, S_C is circular surface of same area as droplet image centred on centred of gravity of the droplet image

Results and discussion

The accurate estimation of droplet volume and droplet external area by the discrete revolution method requires accurate assessment of volume and surface area integration errors, which are inherent to this method. The integration errors are dependent on a number of slices, which are used to represent a droplet and the diameter of the droplet. It is convenient to use a computer generated perfectly spherical droplet and compute external surface area and droplet volume by using the discrete revolution method. It can then be compared with analytical solution for the volume and surface area, which are known *a priori*. Figure 2 shows a computer generated image of a circle with diameter of 100 pixels and the reconstructed 3D shape of a 'digital droplet', which was performed by using the discrete revolution method and 20 slices.

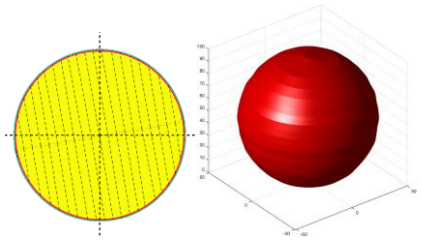

Figure 2: Example of computer generated image of a circle (left). Diameter of the circle is 100 pixels. Reconstructed 3D shape (right) was performed by using discrete revolution method and 20 slices. Note that for reconstructed 3D shape, z-axis is always along droplet major axis.

Depending on a number of slices, the reconstructed shape can be the so-called 'smooth' or 'serrated' even though, the resulting integration errors are weakly dependent on a number of slices. In order to investigate the relationship between the integration error and a droplet diameter, a set of tests was carried out on computer generated perfectly spherical droplets. The perfectly spherical droplets were obtained by revolving a computer generated 2D circles. Figure 3 shows external surface area and computed volume computational errors for a range of computer generated perfectly spherical droplets by using discrete revolution method with 5 slices. Figure 4 shows the same computational errors for the same range of computer generated droplets by using discrete revolution method with 10 slices. All integration errors were computed as follows:

$$\varepsilon_V = \frac{V_a - V_r}{V_a} \cdot 100\%$$
$$\varepsilon_A = \frac{A_a - A_r}{A_a} \cdot 100\% \quad (2)$$

where: ε_V is volume integration error, ε_A is external surface area integration error, A_a is external surface area computed analytically for a droplet of given size, A_r is external surface area computed by using discrete revolution method, V_a and V_r are analytically computed volume and estimated volume by discrete revolution method correspondingly.

Integration errors of external surface area are weakly dependent on a droplet size and asymptotically increase towards 5% value. The discrete revolution method tends to overestimate the true external surface area by 5% in worst case scenario if 5 slices are used to integrate the droplet. For 10 slices, all integration errors were below 5% for all droplet diameters. It should be noted that for a typical microscopy experiment, the scale factor is 0.5-0.6 mm/pixel. Therefore, a typical droplet would be in the range of 60 – 150 pixels. However, volume integration errors are highly dependent on a number of slices as it can be seen in Figures 3 and 4. Volume integration errors for 10 slices were also below 5% in worst case scenario. Therefore, in this work, 10 slices were used in post-processing of all experimental images. It should also be noted that a higher number of slices can be used if necessary. However, computational time significantly increases if several droplets are analyzed at the same time. Larger number of slices was also investigated and no significant improvement in integration was

found. Therefore, the minimum number of slices was chosen on a basis of acceptable integration errors and computational time.

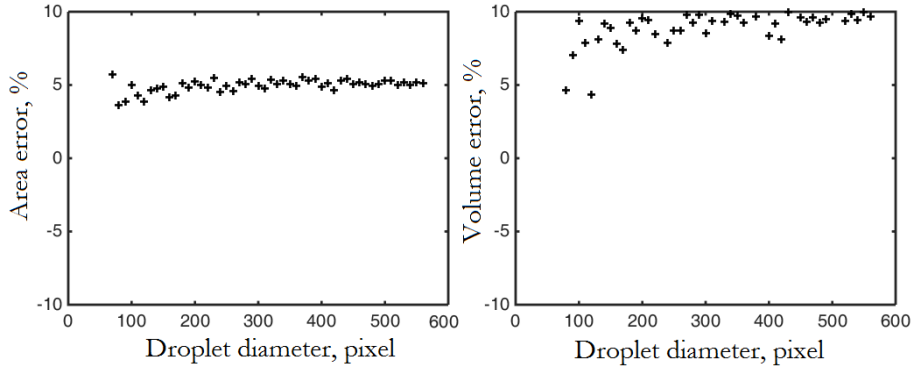

Figure 3: Area (left) and volume (right) computational error (%) for a range of computer generated perfectly spherical droplets for 5 slices. Area and volume of droplets were computed analytically and by using discrete revolution method.

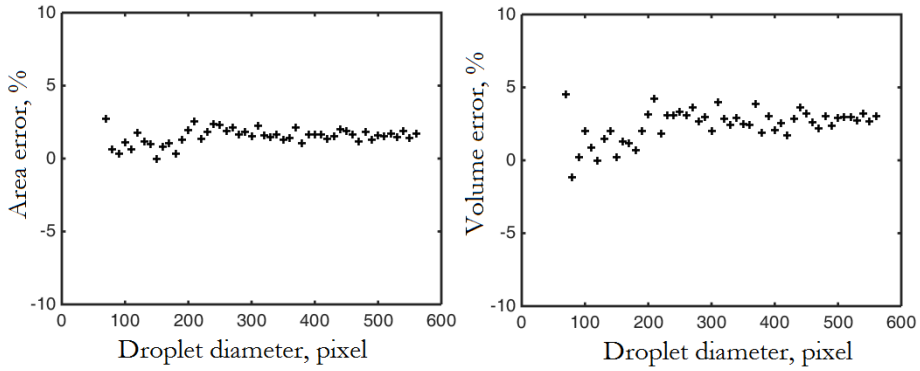

Figure 4: Area (left) and volume (right) computational error (%) for a range of computer generated perfectly spherical droplets for 10 slices. Area and volume of computer generated droplets were computed analytically and by using discrete revolution method.

Figure 5 shows 16 enhanced flat-fielded images obtained using the SIM16 ultra-high speed camera. The injector nozzle is seen as a black region on top right. Raw images obtained from the camera usually have very low contrast ratio and binarisation is hardly possible. Intensified cameras are notoriously known for low signal-to-noise ratio and images obtained with intensified cameras often need to be enhanced. In this research, images were enhanced by using downsampling by 2 and a median filter with kernel of 3x3 pixels. Image enhancing was performed in order to binarise images by using a thresholding method. The quality of the images significantly increased when enhancing was applied.

At time 0 a large droplet with diameter of circa 194 µm and a ligament of 243 µm long are visible. The large droplet slowly moves away from the injector nozzle, while ligament is shrinking with velocity of circa 2.27 m/s (velocity vector is along the major axis of the shrinking ligament). As the ligament shrinks its shape changes to a dumbbell-like structure and eventually becomes nearly spherical droplet during 70 µs. In fact, it is hard to see at time 0 whether the ligament is connected to the large droplet or is separated by a small distance. Droplet shape changes at time 75 µs and resembles oblate spheroid and perhaps starts oscillating after this time (start of oscillation can be seen as the deformation of the droplet shape).

Figure 6 shows computed volume and external surface area for a forming droplet. The volume and external area were computed from time 50 µs (Fig. 5). No binarisation was possible before time 50 µs due to refraction, which had the same intensity as the background and hence, droplet perimeter, volume and external area could not be estimated. Under room ambient conditions no evaporation takes place and hence, the estimated volume must be constant. However, the discripancy in estimated volume reaches 20% (Fig. 6), which can be linked to image binarisation errors. External surface area increases reaching maximum at 70 µs (nearly spherical droplet) and decreases after 70 µs.

Figure 7 shows enhanced flat-fielded images of oscillating droplet of the equivalent diameter of 105 µm found at the end of injection. The most spherical shape of the droplet is found at the time of 15 µs in frame 4, for which sphericity parameter is the lowest (S_p=0.052). The sphericity parameter for a droplet shown in Figure 7 and a droplet in Figure 5 is shown in Figure 8 as a function of time.

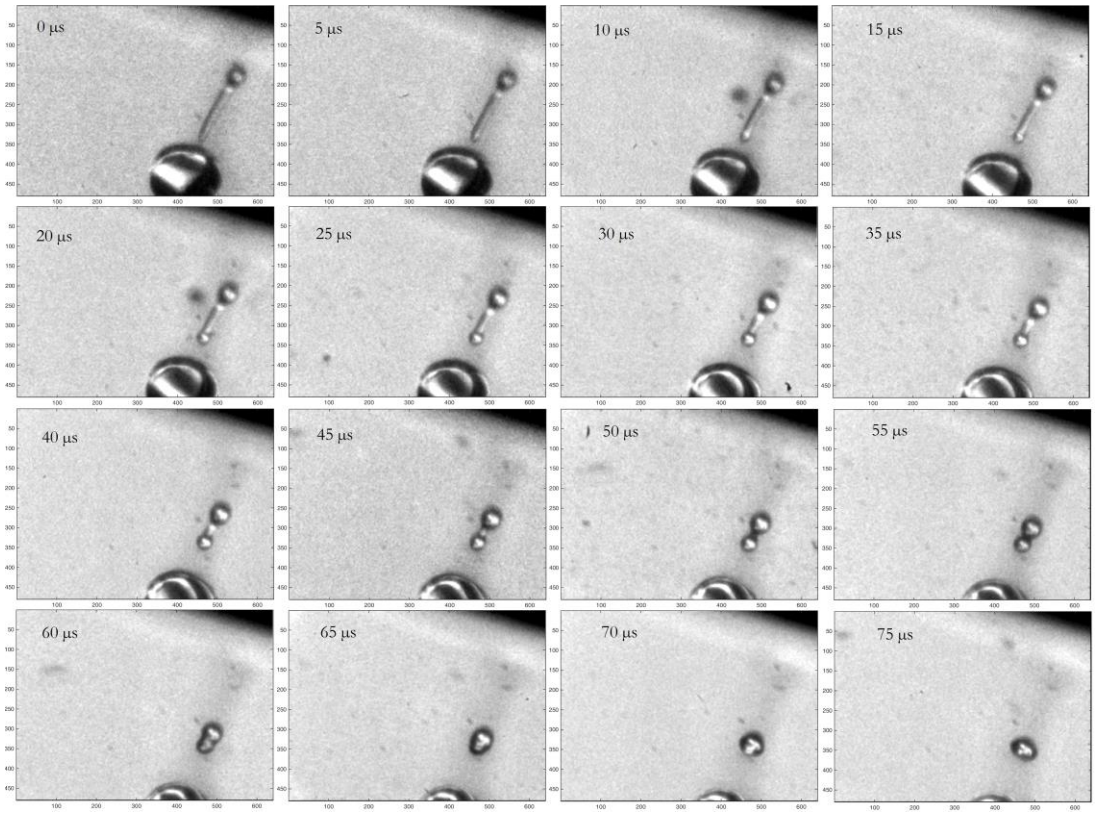

Figure 5: Enhanced flat-fielded images obtained from SIM16 ultra-high speed camera. Images were enhanced by using downsampling by 2 and a median filter with kernel of 4x4 pixels. Equivalent diameter of a nearly spherical droplet formed at time 70 µs is 34 µm. Scale factor is 0.56 µs/pix. Note that enhanced images were downsampled and all pixel coordinates must be multiplied by 2 to correct for downsampling. The ligament shrinks with velocity of circa 2.27 m/s (velocity vector is along the major axis of the shrinking ligament). Fuel is injected at 500 bar under room temperature and pressure ambient conditions.

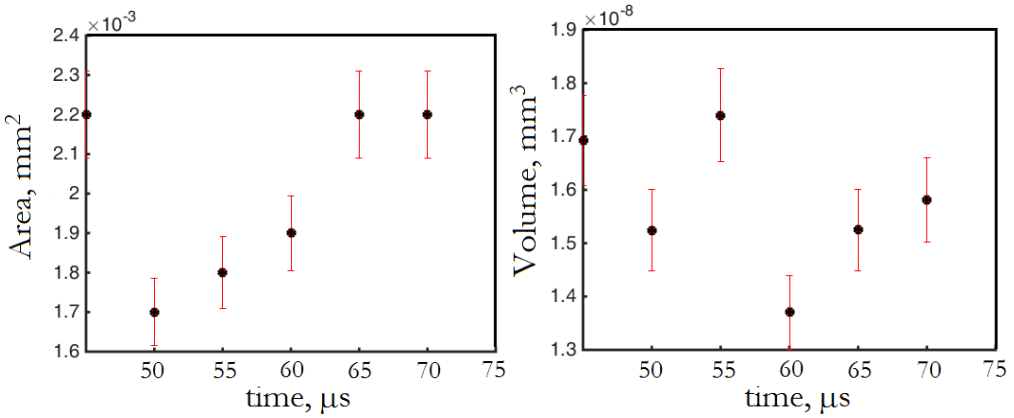

Figure 6: Computed volume (left) and external surface area (right) for a forming droplet, which is shown in Figure 5 by using discrete revolution method. Error bars show ±5% integration errors. No binarisation was possible before time 50 µs due to refraction, which had the same intensity as the background and hence, droplet perimeter could not be estimated.

Computed volume and external surface area for a droplet shown in Figure 7 is also shown in Figure 9. The most spherical shape was used as a benchmark for analytical computation of volume and external surface area. The most spherical shape implies that the droplet projected area can be used in an analytical computation of droplet volume and surface area. Since, the reconstructed volume performed by the discrete revolution method is not constant it can imply that there is a significant change in the shape of the droplet out of the measuring plane. This assumption seems to be plausible, because the droplet is a 3D object and oscillates along all the coordinates,

under the assumption of non-evaporating conditions. It is, therefore, apparent that there is a need for dual camera visualisation technique, e.g. for more accurate droplet shape, volume and surface area estimation and characterization of possible morphological errors in estimation of the 'true' volume and the 'true' surface area.

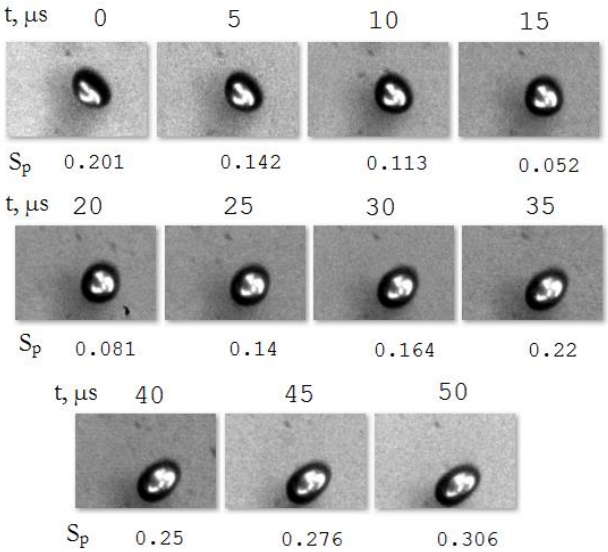

Figure 7: Enhanced flat-fielded images of an oscillating droplet of the equivalent diameter of 105 μm found at the end of injection. Time is plotted on the top of individual frame images and shown in μs. Sphericity parameter computed according to [18] is also shown under each frame image. The most spherical shape is found at the time of 15 μs (S_p=0.052). The absolute velocity of this droplet is circa 3 m/s. Fuel is injected at 500 bar under room temperature and pressure ambient conditions.

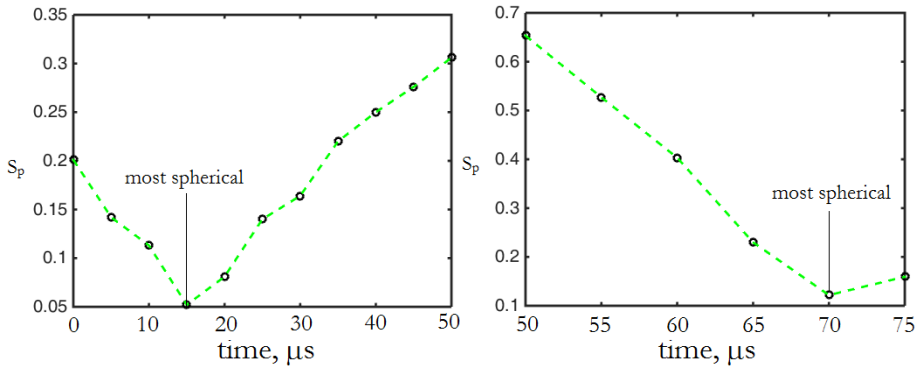

Figure 8: Sphericity parameter as a function of time for a droplet shown in Figure 7 (left) and a droplet in Figure 5 (right).

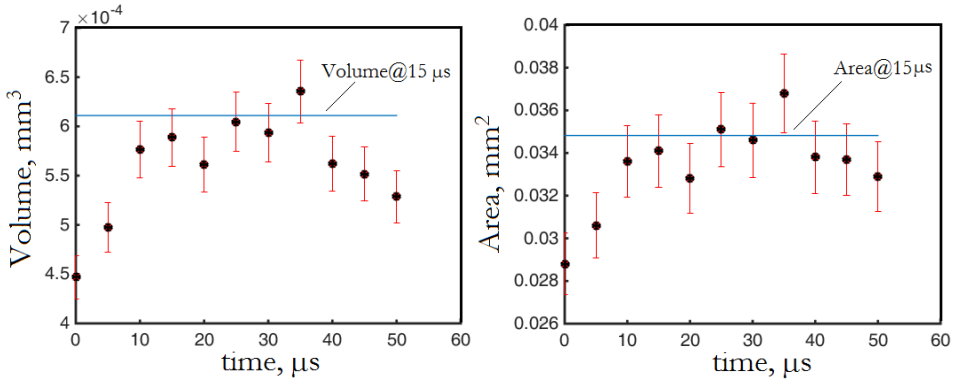

Figure 9: Computed volume (left) and external surface area (right) for a droplet shown in Figure 7 by using discrete revolution method. Error bars show ±5% integration errors. Straight line is the volume and area computed from the most spherical shape of the droplet for which the droplet equivalent diameter was used in analytical evaluation of droplet volume and surface area.

Conclusions

The present work focused on morphological analysis of diesel fuel droplets under primarily atmospheric operating conditions. It was found that:

- Droplet oscillations can be significant and accurate prediction of the droplet volume and external surface area requires utilisation of double camera configuration.
- Large droplets with a diameter bigger than the injector nozzle hole can be formed under atmospheric operating conditions. The large droplet was not analysed in details. However, no significant change in the shape of the large droplet was noticed.
- It was shown that it was possible to reconstruct the 3D shape of the measured droplets by using the discrete revolution method with maximum integration errors of 5% in worst case scenario.
- In high-speed video sequences at non-evaporating conditions, sphericity parameter can in principle be an indicator of change in droplet volume due to out-of-measuring plane droplet oscillation. However, this statements needs to be proved against more rigorous experimental data under better controlled operating conditions, e.g. by using a droplet generator and the two camera configuration.

Acknowledgement

The authors would like to thank BP Formulated Products Technology and the EPSRC (EP/K020528/1) for financial support. The EPSRC Engineering Instrument Pool is also acknowledged for supplying equipment.

References

[1] Patterson, M. A. and Reitz R. D., 1998, SAE Technical Paper 980131.
[2] Arcoumanis, C. and Gavaises, M., 1998, Atomization Sprays 8, pp. 307–347.
[3] Choi, C. Y. and Reitz R. D., 2000, Combust. Sci. Technol. 159, pp. 169–198.
[4] Siebers, D. and Higgins, B., 2001, SAE Technical Paper 2001-01-0530.
[5] Higgins, D. and Siebers, D. L., SAE Paper No. 2001-01-0918, 2001.
[6] Yi, Y. and Reitz, R. D., SAE Paper No. 01-1041, 2003.
[7] Sjoberg, H., et al., 1996, Optical Engineering, 35(12), pp. 3591-3596.
[8] Lai, M.-C., et al., 1998, SAE 982542.
[9] Linne, M. A., et al., 2009, Proceedings of the Combustion Institute 32, pp. 2147–2161.
[10] Linne, M, et al., 2010, Experiments in Fluids, 49(4), pp. 911–923.
[11] Shoba, T. T. et al., 5-7 September 2011, 24th European Conference on Liquid Atomization and Spray Systems, Estoril, Portugal.
[12] Hardalupas Y, Taylor A, Whitelaw J., H., 1992, Int. J. Multiphase Flow 15(2), pp. 159–179.
[13] Gulder, OL. and Smallwood G., J., September 12-15 1999, 4th Int. Conference ICE2001 Internal Combustion Engines: Experiments and Modelling, Capri-Naples, Italy, pp. 497–504.
[14] Stetsyuk, V., et al., September 8-10 2014, 26th Annual Conference on Liquid Atomization and Spray Systems, Bremen, Germany.
[15] Crua, C., et al., September 2-6 2012, 12th Int. Conference on Liquid Atomization and Spray Systems Heidelberg, Germany.
[16] Glenn G., et al., 1993, Aerosol Science and Technology, 19:2, pp. 199-212.
[17] Dumouchel, C., et al., 2010, Part. Part. Syst. Charact. 27, pp. 76–88.
[18] Blaisot, J. B. and Yon, J., 2005, Experiments in Fluids 39, pp. 977–994.
[19] Fdida, N. and Blaisot, J. B., 2010, Meas. Sci. Technol. 21.
[20] Fansler, T. D. and Parrish, S. E., 2015, Meas. Sci. Technol. 26.
[21] Crua, C., Heikal, M.R., and Gold, M.R., 2015, Fuel (in press), http://dx.doi.org/10.1016/j.fuel.2015.04.041